ISSN (Online) 2395-2717

International Journal of Engineering Research in Electrical and Electronic Engineering (IJEREEE)

Volume 12, Issue 8, August 2025

Anti-Reflective Coatings in Photovoltaic and Optical Systems

[1] Subodh Kumar*, [2] Sohini P.

[1] [2] B.Tech., in Engineering Physics, Department of Applied Physics, Delhi Technological University, New Delhi, India
Corresponding Author Email: [1] subodhkumar_ep21b9_79@dtu.ac.in, [2] sohinipurkayastha_2k22ep501@dtu.ac.in

Abstract*— This study examines anti-reflective coatings (ARCs), tracing their development from foundational principles to advanced applications in photovoltaic and optical systems. It begins by outlining the physics of thin-film interference and refractive index matching, establishing the quarter-wave condition and geometric mean refractive index criteria as essential for minimizing surface reflections. Building upon this framework, the implementation of single-layer and multilayer dielectric stacks—composed of materials such as magnesium fluoride, silicon dioxide, and titanium dioxide—is explored for enhancing light transmission and power conversion efficiency in crystalline silicon heterojunction solar cells. Subsequent analysis centers on perovskite solar cells, wherein front-surface ARCs play a critical role in improving photon absorption, protecting moisture-sensitive layers, and enhancing operational stability, particularly in ultra-thin absorber configurations. ARC strategies are further examined in the context of precision optical instruments, including eyeglasses, camera lenses, microscope objectives, and touchscreen displays. Emphasis is placed on material selection and deposition techniques—such as physical vapor deposition, atomic layer deposition, sol-gel processing, and dry etching—that achieve sub-1% reflectance across diverse substrates. In addition, the study underscores the significance of biomimetic nanostructures, inspired by moth-eye surface patterns, in achieving broadband and angle-insensitive anti-reflective performance. It concludes by outlining future directions for ARCs, including the development of multifunctional, environmentally sustainable, and dynamically adaptive "smart" coatings that incorporate features such as self-cleaning, hydrophobicity, and spectral tuning to enhance the performance and sustainability of next-generation optical and photovoltaic technologies.

Keywords: ARCs, optical efficiency, refractive indices, simulation-based design, surface coatings, perovskite, deposition techniques, solar cells.

I. INTRODUCTION

Solar cells, as the cornerstone of photovoltaic technology, convert sunlight into electricity by leveraging the photoelectric effect [1]. However, one of the significant challenges in maximising their efficiency lies in minimising optical losses. A considerable fraction of sunlight is reflected off the surface of the cells due to differences in the refractive indices of air and the photovoltaic material [2] [3]. Anti-reflective (AR) coatings play a crucial role in mitigating these losses, enhancing light absorption, and consequently improving energy conversion efficiency [4].

A. Background and Historical Development

The concept of reducing surface reflection using anti-reflective coatings originated in optical systems, with early applications in lenses and telescopes during the early 20th century. Inspired by nature—such as the eyes of moths, which have nano-structured anti-reflective surfaces—researchers developed coatings that manipulate incident light through interference effect [5].

The integration of AR coatings into photovoltaic technologies began in the mid-20th century, as researchers sought to enhance the efficiency of solar cells [6] [7]. Initial efforts focused on single-layer coatings composed of materials such as silicon nitride and magnesium fluoride, which provided partial reflection reduction for specific wavelengths of light. As photovoltaic technologies advanced, so did the requirements for AR coatings, leading to the development of multi-layer and gradient-index coatings that optimise performance across the solar spectrum [8].

With the advent of nanotechnology, techniques such as etching and deposition allowed for the fabrication of nano-structured surfaces that mimic natural anti-reflective properties. These advances not only improved light absorption but also introduced self-cleaning properties, further enhancing the durability and efficiency of solar cells [9].

B. Basic Concept

Anti-reflective coatings (ARCs) are crucial in minimising the reflection of light at material surfaces, enhancing the efficiency of solar cells by maximising the amount of light transmitted into the active layers.

1. Reflection at an Interface

When light encounters a boundary between two materials with different refractive indices, some of it is reflected back. The amount of reflected light is quantified using the Fresnel equation for normal incidence:

$$R = \left(\frac{n_1 - n_2}{n_1 + n_2}\right)^2$$

where:

n_1 is the refractive index of the medium the light originates from (e.g., air, typically n_1=1.0).

ISSN (Online) 2395-2717

International Journal of Engineering Research in Electrical and Electronic Engineering (IJEREEE)

Volume 12, Issue 8, August 2025

n_2 is the refractive index of the material the light is entering (e.g., silicon or glass) [10].

2. *Thin Film Interference*

To reduce this reflection, ARCs use thin-film interference, where a coating layer is applied to the surface. Reflections from the top and bottom surfaces of the coating can interfere destructively, canceling each other out.

This destructive interference is achieved when the phase difference between the reflected waves is exactly π radians (or half a wavelength). The condition for this to occur is:

$$d = \frac{\lambda}{4n}$$

where:
d is the thickness of the coating,
λ is the wavelength of the incident light,
n is the refractive index of the coating [11].

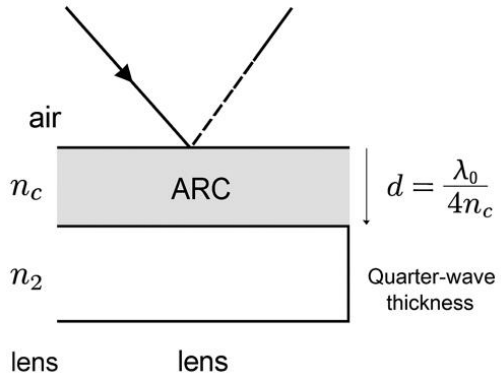


Fig. 1 Diagram illustrating the lens configuration along with the quarter-wave condition for a design wavelength

3. *Optimal Refractive Index*

The ideal refractive index of the coating material is chosen to further minimise reflection. For a single-layer coating, the optimal refractive index nc is the geometric mean of the refractive indices of the surrounding air (nair) and the substrate (ns):

$$\boldsymbol{n_c = \sqrt{n_{air} \cdot n_s}}$$

For air (nair=1.0) and silicon (ns=3.5), the optimal coating refractive index is:

$$\boldsymbol{n_c = \sqrt{1.0 \cdot 3.5} \approx 1.87}$$

This value ensures the best match for minimising reflectance at the specified wavelength.

4. *Reflectance Reduction*

The effectiveness of an ARC is evaluated by the residual reflectance R_{ARC}, which depends on the refractive index match between the air, the coating, and the substrate. With the optimal refractive index n_c, the reflectance at normal incidence is significantly reduced compared to an uncoated surface [12].

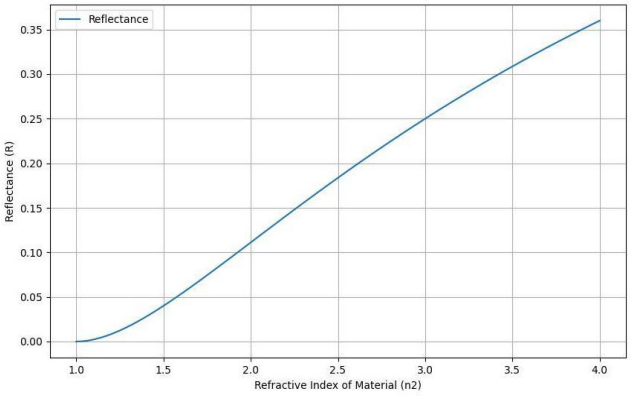


Fig. 2 Reflectance v/s Refractive Index of Coating Material

C. Overview of Heterojunction Cells

Silicon heterojunction (HJT) solar-cell technology has its roots in the 1970s, when researchers first recognised that depositing thin amorphous silicon (a-Si) films onto crystalline silicon (c-Si) substrates could serve both as a junction and an effective surface-passivation layer. By 1983, efficiencies exceeding 12 % were reported for early a-Si/c-Si heterojunction devices, and in the early 1990s Sanyo (now part of Panasonic) introduced the "Heterojunction with Intrinsic Thin-layer" (HIT) cell, adding intrinsic hydrogenated a-Si:H (i-a-Si:H) layers to reduce interface recombination and dark leakage currents [13]. Although proprietary patents briefly constrained wider adoption, the expiration of these patents in 2011 unleashed rapid innovation. Panasonic achieved over 25 % conversion efficiency in 2014, Kaneka reached 26.7 % in 2018, and LONGi set a new record of 27.09 % in early 2023, making HJT the most efficient non-concentrator silicon technology to date . Global production capacity has since scaled to the gigawatt level, with more than twenty manufacturers—such as Huasun, Risen, and Meyer Burger—ramping HJT lines for both monofacial and bifacial modules [14].

At their core, HJT cells juxtapose thin intrinsic a-Si:H layers on both sides of an n- or p-type c-Si wafer to achieve exceptional surface passivation and low recombination velocities . Doped a-Si:H emitter layers then establish the heterojunction, while transparent conductive oxides (TCOs) like indium-tin oxide serve simultaneously as low-loss optical coatings and carrier-collecting electrodes. Screen-printed metal grids complete the front and rear contacts, balancing minimal shading with efficient current extraction [15]. This architecture harnesses the wide bandgap of a-Si:H to suppress surface-recombination losses, retains the high bulk lifetime and mobility of crystalline silicon for strong carrier collection, and naturally supports bifacial energy generation under albedo light, yielding high open-circuit voltages (V_oc), elevated fill factors, and superior thermal stability compared to conventional homojunction cells.

ISSN (Online) 2395-2717

International Journal of Engineering Research in Electrical and Electronic Engineering (IJEREEE)

Volume 12, Issue 8, August 2025

D. Overview of Perovskite Solar Cells

Perovskite solar cells (PSCs) have emerged as transformative technologies in the field of photovoltaics, owing to their exceptional optoelectronic properties and facile fabrication processes. Characterised by an ABX_3 crystal structure, these materials offer a unique combination of high absorption coefficients, long carrier diffusion lengths, tuneable band-gaps, and compatibility with both single-junction and tandem cell architectures. Their potential for low-cost, solution-based manufacturing and compatibility with flexible substrates positions them as strong candidates for next-generation solar energy systems, offering an attractive alternative to traditional silicon-based devices.

A typical PSC is composed of a transparent conductive oxide (TCO), an Electron Transport Layer (ETL), a perovskite absorber layer, a Hole Transport Layer (HTL), and a back electrode. Device performance critically depends on the optimal alignment of energy levels between these layers and the perovskite material. Given the ultra-thin nature of perovskite layers, typically less than 1 µm, maximising light absorption becomes vital for efficient carrier generation.

Anti-Reflective Coatings (ARCs) play a crucial role in enhancing PSC performance by minimising front-surface reflection, particularly in the UV-visible spectrum, thereby allowing a greater fraction of incident photons to reach the active layer. Beyond optical enhancement, ARCs serve to protect the sensitive perovskite layer from environmental factors such as moisture and UV-induced degradation, thereby contributing to improved operational stability.

The term "perovskite" originally referred to a naturally occurring mineral, calcium titanate ($CaTiO_3$), discovered in 1839 by German mineralogist Gustav Rose and named in honour of Russian mineralogist Lev Perovski. The term later came to denote a class of materials with the same crystal structure (ABX_3), where:

A = organic/inorganic cation (e.g., methylammonium)

B = metal cation (e.g., Pb^{2+})

X = halide anion (Cl^-, Br^-, or I^-) [16].

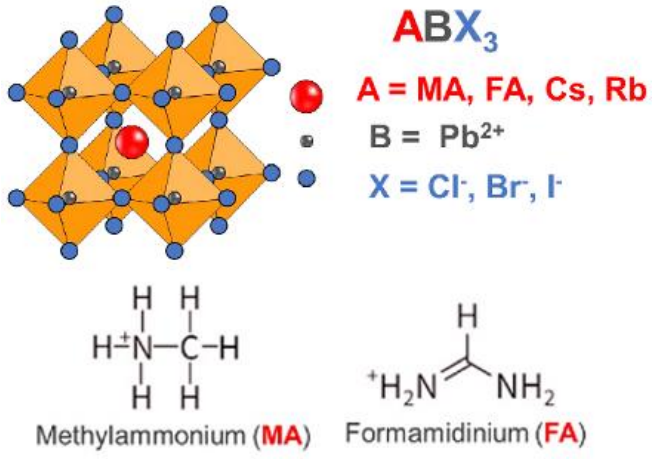


Fig. 3 Crystal Structure of Perovskites [17]

The first notable application of perovskite materials in solar cells was demonstrated by Miyasaka et al. in 2009, achieving a power conversion efficiency (PCE) of 3.8% using methylammonium lead halides in a dye-sensitised configuration. However, rapid degradation due to the use of liquid electrolytes initially limited their stability. A major breakthrough came in 2012 when solid-state hole transport materials replaced liquid electrolytes, significantly enhancing device stability and pushing efficiencies above 10% [18]. Since then, PSCs have witnessed rapid advancements through improved layer architectures, doping of charge transport layers, and interface passivation strategies. Single-junction perovskite devices have now achieved certified efficiencies exceeding 25%, while tandem configurations integrating perovskites with silicon or other absorbers have surpassed 33%, exceeding the theoretical Shockley-Queisser limit for single-junction cells.

The appeal of perovskite-based photovoltaics is further strengthened by their low-temperature processing, scalability, and compatibility with lightweight, flexible substrates. These features open pathways for applications in wearable electronics, building-integrated photovoltaics (BIPV), and portable power solutions. As research continues to advance, the strategic integration of anti-reflective coatings will be critical to optimising light management, enhancing device stability, and supporting the commercialisation of perovskite solar technologies [19].

II. LITERATURE REVIEW

The concept of anti-reflective coatings (ARCs) can be traced to the mid-19th century through the observations of Lord Rayleigh, who noted that aged, tarnished optical glass exhibited greater light transmission compared to pristine, untarnished samples. This phenomenon was attributed to the formation of a thin tarnish layer on the glass surface, which introduced two interfaces—air-tarnish and tarnish-glass—instead of a direct air-glass interface. As the tarnish possessed a refractive index intermediate between air and glass, each interface reflected less light than the original air-glass boundary. Rayleigh's insights provided an early understanding of how surface modifications could manipulate optical properties, laying the groundwork for later developments in thin-film interference technologies.

A significant technological leap occurred in 1935 when Olexander Smakula, working for Carl Zeiss optics company, developed the first systematic interference-based ARC. Initially kept as a classified German military secret during World War II, Smakula's work introduced a deliberate and engineered approach to reducing surface reflections, extending far beyond the natural tarnish phenomena observed by Rayleigh. After the war, these advancements became widely known and formed the foundation for modern anti-reflective technologies used in optics, photovoltaics, and display systems [20].

ISSN (Online) 2395-2717

International Journal of Engineering Research in Electrical and Electronic Engineering (IJEREEE)

Volume 12, Issue 8, August 2025

The most basic anti-reflective coatings are single-layer designs, comprising a thin, transparent material whose refractive index is chosen as the geometric mean between air ($n \approx 1.0$) and the substrate, such as optical glass ($n \approx 1.52$). For crown glass, this theoretical ideal index is approximately 1.23. Although materials with precisely this refractive index are rare, magnesium fluoride (MgF_2), with a refractive index of about 1.38, has proven to be an effective and practical choice due to its optical clarity, durability, and ease of deposition. Fluoropolymers, offering even lower refractive indices (~1.30), are also employed, though their use is limited by more challenging processing requirements.

Despite their simplicity, single-layer ARCs are inherently constrained by their narrowband optimisation. They are most effective only at a specific wavelength and angle of incidence, resulting in suboptimal performance for broadband light sources or systems subjected to varying angles of illumination. This limitation prompted the evolution of multi-layer anti-reflective coatings, which utilise alternating layers of materials with high and low refractive indices to broaden the effective bandwidth and angular response. By carefully engineering the thicknesses and material choices of each layer, multi-layer ARCs achieve significantly improved suppression of reflections, reaching reflectivities as low as 0.1% at target wavelengths.

Material selection is critical for multi-layer ARC performance. High-index materials, such as titanium dioxide (TiO_2, $n \approx 2.2–2.5$ in the visible spectrum), tantalum pentoxide (Ta_2O_5, $n \approx 2.1$), and zinc sulphide (ZnS, $n \approx 2.3$), offer strong optical contrast when paired with low-index materials like silicon dioxide (SiO_2, $n \approx 1.45$), magnesium fluoride (MgF_2, $n \approx 1.38$), or aluminium oxide (Al_2O_3, $n \approx 1.6$). The refractive index contrast between adjacent layers is crucial for achieving effective destructive interference and minimising reflectance. Higher contrast leads to greater reflection suppression, but it also complicates the fabrication process, requiring precise control over film thickness and deposition uniformity [21]. The production of multi-layer ARCs introduces considerable technical and economic challenges. Complex stacking sequences and tighter tolerances on layer thicknesses necessitate advanced fabrication techniques, such as physical vapour deposition (PVD), atomic layer deposition (ALD), and chemical vapour deposition (CVD). The need for meticulous control significantly increases production costs, limiting the widespread use of sophisticated multi-layer coatings in cost-sensitive sectors. Moreover, ensuring long-term adhesion and mechanical integrity across multiple layers adds further design constraints, particularly for applications exposed to environmental stresses.

Although traditional ARCs have enabled significant advancements across optical and energy applications, they exhibit inherent limitations that restrict their broader adaptability. One key challenge is their wavelength specificity; most designs are optimised for a particular range of the electromagnetic spectrum, such as visible, ultraviolet, or infrared. Applications requiring broadband performance—such as solar panels, imaging optics, or multi-spectral sensing—often find conventional ARCs insufficient. Although multi-layer architectures improve spectral coverage, they do so at the cost of greater fabrication complexity and mechanical vulnerability [22].

Another notable limitation is the strong angular dependence of ARC performance. While coatings perform optimally under normal (perpendicular) light incidence, their effectiveness diminishes as the angle of incoming light deviates. This angular sensitivity is particularly problematic for systems like photovoltaic cells, where incident sunlight varies significantly throughout the day, or for wide-angle imaging systems requiring consistent optical performance across broad fields of view.

Environmental durability also remains a critical concern. ARCs exposed to outdoor or high-stress environments must withstand temperature fluctuations, humidity, ultraviolet radiation, and physical wear. Many conventional coatings, particularly those relying on brittle materials or complex multi-layer stacks, are prone to degradation mechanisms such as delamination, cracking, or refractive index shifts, ultimately compromising optical performance and reducing device longevity. Thus, the development of more robust and multifunctional coatings—combining anti-reflective properties with hydrophobicity, anti-fogging, or self-cleaning functionalities—has become a growing research priority [23].

In parallel, perovskite solar cells (PSCs) have emerged as a highly promising photovoltaic technology due to their exceptional power conversion efficiencies and low-cost fabrication potential. Nevertheless, several major challenges hinder their reliable commercial deployment. Material stability remains a pressing issue; perovskites are highly sensitive to moisture, oxygen, thermal stress, and ultraviolet radiation, leading to rapid performance degradation under ambient conditions. Ion migration within the perovskite layer induces hysteresis effects in current-voltage measurements and accelerates device instability over time.

Interface engineering is another critical bottleneck. Imperfect contact between the perovskite absorber and the electron and hole transport layers (ETL and HTL) promotes non-radiative recombination losses, reducing open-circuit voltage and fill factor. Defect states, particularly at grain boundaries, introduce trap-assisted recombination pathways, further undermining carrier lifetimes and overall device performance. In addition, the presence of lead in most high-efficiency perovskite compositions poses significant environmental and health concerns, prompting the search for effective encapsulation strategies or the development of lead-free perovskite alternatives [24].

Scaling perovskite solar technology from laboratory cells to large-area modules introduces further complexities, including maintaining film uniformity, interface integrity,

ISSN (Online) 2395-2717

International Journal of Engineering Research in Electrical and Electronic Engineering (IJEREEE)

Volume 12, Issue 8, August 2025

and device reproducibility over larger surfaces. Doping strategies, while offering potential benefits such as enhanced charge mobility and improved energy alignment, must be precisely controlled to avoid introducing unwanted defect states or phase instabilities.

Flexible thin-film solar cells represent a particularly exciting application space for perovskites, offering opportunities in wearable electronics, portable energy systems, and flexible displays. Their light weight, mechanical flexibility, and low-temperature processability (below ~150 °C) make perovskites particularly well-suited for integration onto flexible polymer substrates such as polyethylene terephthalate (PET). Flexible PSCs have been realized using both n-i-p and p-i-n device architectures, employing ETM/perovskite/HTM or HTM/perovskite/ETM stacking sequences, respectively. Conventional high-temperature ETMs such as TiO_2 have prompted a preference for p-i-n configurations, using low-temperature processed materials like PEDOT:PSS and PCBM.

Recent progress has also enabled n-i-p structured flexible devices by employing alternative ETMs like ZnO nano-materials, which can be deposited below 150 °C. Kelly et al. demonstrated a flexible n-i-p perovskite solar cell with a power conversion efficiency (PCE) of 10.2%, while more recent advances employing TiOx layers deposited via atomic layer deposition (ALD) have pushed flexible PSC efficiencies beyond 12%. Flexible perovskite solar cells remain in their early stages of technological maturity, offering significant potential for future innovation in materials science, device engineering, and scalable manufacturing techniques [25].

III. THEORETICAL BASIS OF ANTI-REFLECTIVE COATINGS

Anti-reflective coatings work by reducing light reflection through the mechanism of destructive interference. When light passes through a thin dielectric layer applied to a solar cell, the reflections from the top and bottom surfaces cancel each other out if specific conditions are met. This phenomenon ensures that more light enters the solar cell, improving energy absorption. For broadband anti-reflective properties, multi-layer coatings or materials with gradient-index profiles are employed. These configurations allow light to enter efficiently across a wide range of wavelengths [26].

1. Requirements for Effective Anti-Reflectivity

To achieve optimal performance, ARCs must meet specific requirements:

a. Refractive Index Balance:

The refractive index of the coating should be chosen to minimize the mismatch between air and the silicon substrate. This is achieved when the refractive index of the coating (n_{ARC}) is the geometric mean of air (nair=1.) and silicon (nsubstrate≈3.5):

Table 1. Refractive index and corresponding reflectance for commonly used ARC materials [27]

Material	Refractive Index (n)	Reflectance (%) at Air Interface
Magnesium Fluoride (MgF_2)	1.38	4.0
Silicon Nitride (Si_3N_4)	2.0	8.0
Zinc Oxide (ZnO)	2.0	8.0
Titanium Dioxide (TiO_2)	2.4	10.0
Poly (methyl methacrylate) (PMMA)	1.49	5.0
Graphene	2.2	9.0

b. Optimised Thickness:

The coating's thickness should induce destructive interference for wavelengths within the solar spectrum, typically focusing on a central wavelength of around 600 nm.

c. Broadband and Angular Performance:

Multi-layer and gradient-index ARCs provide anti-reflection over a wider range of wavelengths and maintain effectiveness across varying angles of light incidence.

d. Durability:

The materials used must withstand environmental stresses, including UV radiation, temperature fluctuations, and humidity [28].

2. Heterojunction Cells

Heterojunction solar cells are a class of photovoltaic devices that utilise a junction formed between two dissimilar semiconductor materials—typically differing in band-gap, doping type, or crystal structure—to enhance charge separation and carrier collection. Their architectures are particularly advantageous for minimizing recombination losses, enabling low-temperature processing, and achieving high open-circuit voltages. Their compatibility with advanced light-trapping structures and passivation techniques makes them a strong candidate for next-generation high-efficiency solar technologies.

a. Classification of ARCs by Layer Design

ARCs utilise multiple layers of materials to achieve broadband anti-reflectivity. Each layer has a specific refractive index and thickness to induce destructive interference across a wide range of wavelengths [29].

ISSN (Online) 2395-2717

International Journal of Engineering Research in Electrical and Electronic Engineering (IJEREEE)

Volume 12, Issue 8, August 2025

- *Single-Layer ARCs (SLARCs)*

A single-layer ARC consists of one dielectric material. The refractive index (n_{SLARC}) is chosen as the geometric mean of air (n_{air}) and silicon ($n_{substrate}$):

$$n_{SLARC} = \sqrt{1.0 \cdot 3.5} \approx 1.87$$

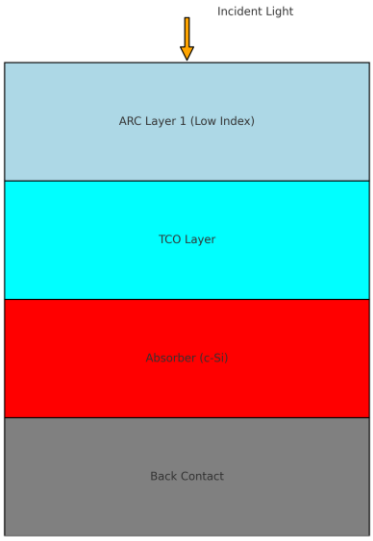


Fig. 4 Schematic Diagram of Single-Layer ARC

The thickness is optimized for a specific target wavelength (λ), typically around 600 nm:

$$d_{SLARC} = \frac{\lambda}{4n_{SLARC}}$$

For $n_{SLARC} = 1.87$:

$$d_{SLARC} = \frac{600nm}{4 \times 1.87} \approx 80.32nm$$

- *Double-Layer ARCs (DLARCs)*

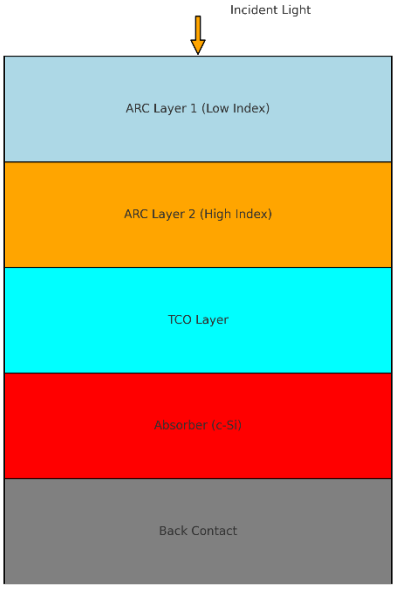


Fig. 5 Schematic Diagram of Double-Layer ARC

Double-layer ARCs utilise two materials with low and high refractive indices (low and high) to expand the anti-reflective range. The optimal design balances the contributions of each layer to destructive interference.

- **Low-Index Layer (e.g., MgF_2)**: $n_{low} \approx 1.38$
- **High-Index Layer (e.g., ZnO)**: $n_{high} \approx 2.0$

- *Triple-Layer ARCs (TLARCs)*

Triple-layer ARCs introduce a third material to further reduce reflectance across a broader spectrum. Materials typically include:

1. **Low-Index Layer (e.g., MgF_2)**: $n_{low} \approx 1.38$
2. **Intermediate-Index Layer (e.g., TiO_2)**: $n_{intermediate} \approx 2.4$
3. **High-Index Layer (e.g., ZnO)**: $n_{high} \approx 2.0$

Thicknesses are calculated for each layer based on the target wavelength range.

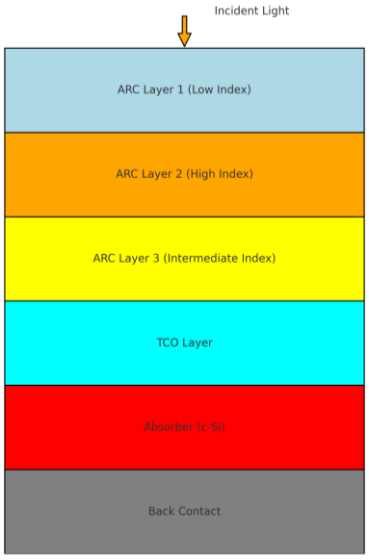


Fig. 6 Schematic Diagram of Multilayer ARC

b. Classification of ARCs by Material

1. Silicon-Based Materials:

Silicon nitride (Si_3N_4) is a common choice due to its dual role as an anti-reflective and passivation layer, protecting the cell from environmental degradation.

2. Metallic Oxides:

- Magnesium Fluoride (MgF_2): A low-index material used in outer layers of multi-layer ARCs.
- Zinc Oxide (ZnO): A high-index material that pairs effectively with MgF_2 for double-layer coatings.
- Titanium Dioxide (TiO_2): Known for its excellent optical properties, particularly in triple-layer designs.

ISSN (Online) 2395-2717

International Journal of Engineering Research in Electrical and Electronic Engineering (IJEREEE)

Volume 12, Issue 8, August 2025

3. Polymer-Based Materials:

Polymers such as PMMA are lightweight, flexible, and ideal for curved solar panels or wearable devices.

4. Nano-structured Materials:

These materials mimic natural designs, such as moth-eye structures, to provide superior broadband performance.

5. Hybrid Coatings:

Combinations of polymers and metallic oxides offer tailored optical and mechanical properties [30].

3. Perovskite-Based Solar Cells and Layer Architecture

Perovskite solar cells (PSCs) have emerged as one of the most promising candidates for next-generation photovoltaics. Their rapid rise in efficiency—from under 4% in 2009 to over 25% in under a decade—has drawn widespread research and industrial interest. A major advantage of perovskite materials is their solution-process ability, which allows fabrication via low-temperature and scalable techniques like spin-coating and inkjet printing, significantly reducing production costs. Structurally, PSCs rely on a multilayer architecture for efficient charge separation and transport.

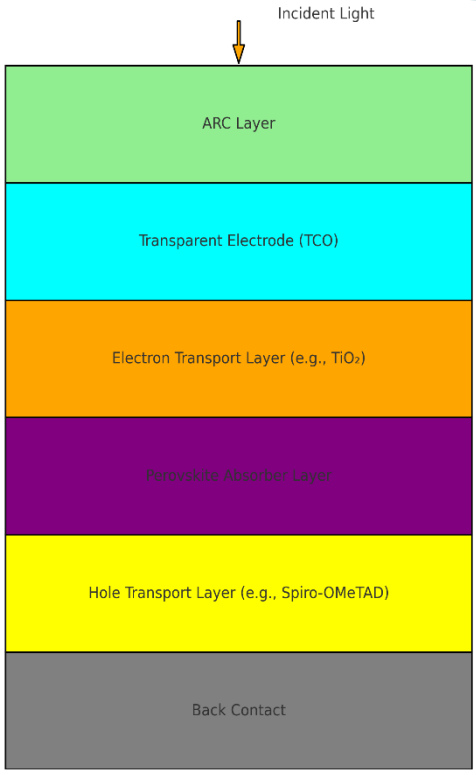


Fig. 7 Schematic Diagram of Perovskite Solar cell with ARC

wo critical components are the Electron Transport Layer (ETL) and the Hole Transport Layer (HTL). The ETL extracts and transports electrons from the perovskite absorber layer to the electrode, while also serving as a barrier to holes. Common ETL materials include titanium dioxide (TiO_2), tin oxide (SnO_2), and [6,6]-phenyl-C_{61}-butyric acid methyl ester (PCBM). On the other hand, the HTL facilitates hole transport and blocks electron flow toward the anode; materials such as Spiro-OMeTAD, nickel oxide (NiOx), and PTAA are frequently employed in this role [31].

The synergy between ETL/HTL materials and the perovskite absorber directly influences parameters like open-circuit voltage (Voc), fill factor (FF), and long-term stability. Anti-reflective coatings can play a transformative role here, particularly in improving light management, enhancing charge carrier generation, and minimising reflection losses across varied wavelengths and angles of incidence. Another pivotal technique in improving PSC efficiency is doping. Intentional introduction of dopants into the ETL, HTL, or even the perovskite absorber layer alters its electrical properties—enhancing conductivity, carrier mobility, and reducing recombination losses. For instance, Li^+ or Co^{++} doped Spiro-OMeTAD in the HTL increases hole mobility, thereby improving charge transport and reducing series resistance. Similarly, doping TiO_2 with metals like Nb or rare-earth elements in the ETL improves electron conductivity and reduces recombination at the interface. Doping can also lead to better band alignment and higher open-circuit voltage (Voc), resulting in increased Power Conversion Efficiency (PCE). In the context of ARC integration, doping can be tuned to work synergistically with optical enhancements—optimising both electrical and optical pathways for efficient energy harvesting.

4. Precision Optical Devices

Anti-reflective coatings (ARCs) for high-precision optics employ the foundational quarter-wave interference principle. At the design wavelength, reflections from the air-film interface and the film-substrate interface cancel destructively, minimising surface reflectance to near zero at normal incidence. To maintain sub-1 % reflectance across broad spectral bands and over incident angles up to 60°, designers turn to multilayer stacks or graded-index nanostructure, each layer or feature tuned to preserve the quarter-wave condition at different portions of the spectrum [32].

Optical ARCs are engineered with a variety of materials and layer configurations, each tailored to the specific demands of different optical devices:

Single-Layer Coatings:

Materials like MgF_2 (with an index near 1.38) are often used on lenses such as those made from CR-39 or polycarbonate. This approach is well-suited for applications where a narrow spectral band is acceptable.

Multilayer Coatings:

For applications requiring wide spectral performance and stable performance over a range of angles (e.g., high-end camera optics, telescope lenses), multilayer stacks are preferred. Typical combinations include alternating layers of low-index materials (MgF_2) and high-index materials (TiO_2

ISSN (Online) 2395-2717

International Journal of Engineering Research in Electrical and Electronic Engineering (IJEREEE)

Volume 12, Issue 8, August 2025

or SiO_2). The design of such stacks is optimised using the transfer-matrix method:

$$M = \prod_{i=1}^{N} \left(\frac{cos\ cos\ \delta_i}{\eta_i\ sin\ sin\ \delta_i} \cdot \frac{\eta_i}{sin\ sin\ \delta_i\ \ cos\ cos\ \delta_i} \right)$$

Where $\delta_i = \frac{2\pi n_i d_i coscos\ \theta_i}{\lambda}$ represents the optical phase of layer i and η_i is its admittance.

Nano-structured and Biomimetic Coatings:

Drawing inspiration from natural phenomena—such as the nano-structured surfaces of moth eyes—novel ARCs incorporate sub-wavelength structures that create a gradual refractive index transition. These coatings can yield ultra low reflectance over both the visible and near-infrared spectra, making them ideal for high-precision applications like microscope objectives and high-definition displays.

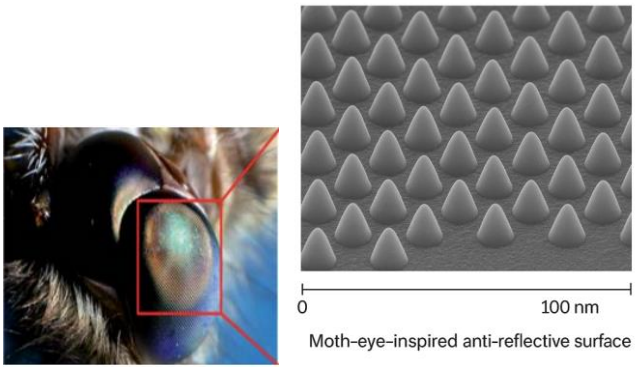


Fig. 8 Moth-eye-inspired nano-structured surface with typical feature sizes in the 0–100 nm range [33]

The choice of fabrication method is dictated by substrate complexity and performance requirements. PVD (e-beam evaporation or sputtering) remains standard for large, flat glass optics. Atomic layer deposition (ALD) delivers pinhole-free, conformal films on curved spectacle and specialty lenses. Sol-gel processing allows low-temperature ARCs on flexible plastics, while reactive ion etching sculpts nano-structured profiles for military and scientific optics.

IV. METHODOLOGY

1. Simulation of Solar Cells

a. Simulation Tool: AFORS-HET

AFORS-HET (Automat FOR Simulation of Heterojunction Solar Cells) is a widely used simulation tool designed for analysing and optimising heterojunction solar cells. It solves the fundamental equations of charge transport, generation, and recombination processes within solar cells. Users can input material-specific parameters such as band-gap energy, carrier mobility, doping density, and defect levels, along with structural characteristics like layer thickness and doping profiles. AFORS-HET is particularly suited for complex architectures involving multi-layers, graded interfaces, and heterojunctions, allowing the simulation of intricate charge carrier dynamics. By integrating physical models with adjustable optical and electrical properties, AFORS-HET enables a comprehensive analysis of device performance, focusing on metrics such as current-voltage characteristics, quantum efficiency, and carrier recombination rates. In this study, AFORS-HET is employed to simulate the baseline performance of perovskite solar cells and assess the influence of different anti-reflective coating (ARC) designs on optical and electrical outputs [34].

b. SCAPS Simulation

SCAPS (Solar Cell Capacitance Simulator), developed at the University of Ghent, is another powerful one-dimensional solar cell simulation tool employed in this work. SCAPS solves the Poisson, electron, and hole continuity equations under steady-state conditions to model the electronic behavior of thin-film solar devices. It offers flexibility in modelling multilayer structures by allowing precise control over layer thicknesses, defect states, interface recombination, and doping levels. SCAPS is particularly adept at modeling materials such as perovskites, CIGS, and CdTe, making it well-suited for evaluating perovskite solar cells' behavior under different conditions. Its ability to simulate device operation under variable illumination, temperature, and bias voltages enables detailed investigation into the influence of ARC integration on device stability and efficiency. SCAPS is used alongside AFORS-HET to cross-validate simulation results and provide a robust analysis framework, minimizing tool-specific biases and ensuring consistency across different modelling approaches.

By combining AFORS-HET and SCAPS, a multi-tool simulation strategy is employed to achieve a comprehensive understanding of material, optical, and electronic impacts arising from ARC modifications [35].

2. Light Trapping vs. Parasitic Absorption: Designing ARCs Without Introducing Losses

While ARCs are primarily introduced to reduce front-surface reflection, their overall effectiveness depends not only on optical design but also on material transparency and energy losses through parasitic absorption. Light trapping is enhanced by promoting multiple internal reflections, thereby increasing the photon path length within the absorber layer. This mechanism becomes particularly critical in ultra-thin perovskite absorbers, where maximizing photon recycling can substantially improve device efficiency.

However, the choice of ARC materials plays a crucial role. Some materials, particularly high-index metal oxides like TiO_2, exhibit notable absorption in the ultraviolet (UV) or infrared (IR) regions. This parasitic absorption decreases the number of photons reaching the active layer, ultimately reducing short-circuit current density and device efficiency. Thus, ARC design must delicately balance refractive index matching, broadband anti-reflection capability, and minimal

ISSN (Online) 2395-2717

International Journal of Engineering Research in Electrical and Electronic Engineering (IJEREEE)

Volume 12, Issue 8, August 2025

parasitic absorption.

Ideal ARCs for perovskite solar cells typically use low-absorption dielectric materials or nanostructured coatings capable of offering broadband anti-reflectivity without significant optical losses. Structures such as nanoporous layers, moth-eye patterns, and multi-layer dielectric stacks are explored to optimize light management. Emphasis is placed on selecting ARC materials that are transparent across the 300–800 nm range where perovskites exhibit strong absorption, thereby ensuring that the integration of the ARC contributes positively to the overall device performance [36].

V. INDUSTRIAL APPLICATIONS OF ARCS

Industrial adoption of anti-reflective coatings (ARCs) spans diverse markets—from high-efficiency heterojunction and perovskite photovoltaics to precision optical instruments. In silicon heterojunction (SHJ) modules, PECVD-deposited silicon nitride (SiNx) and MgF_2 single films reduce front-surface reflection by over 80 %, translating to 3–5 % increases in short-circuit current density (J_s) and 2–5 % annual energy gains in commercial modules [37]. Bilayer stacks (MgF_2/Al_2O_3, Al_2O_3/IZO) and TiO_2/ZnO multilayers extend suppression across 400–900 nm, driving >10 % yield improvements and record SHJ efficiencies above 26 %. In perovskite solar cells (PSCs), sub-micrometer absorbers are paired with spin-coated silica and fluorinated-polymer ARCs, cutting reflectance from ~12 % to <2 % across 400–800 nm and boosting J_s by ~8 %. Nano-patterned honeycomb SU-8 textures and MgF_2/TiO_2 bilayers further raise PCE from 22.7 % to 23.9 %, while enforcing moisture protection that extends T_{80} lifetimes by >200 h at 85 °C/85 % RH . In optical instruments, ARCs employ quarter-wave thin films and graded-index nano structures—single-layer MgF_2, multilayer $MgF_2/TiO_2/SiO_2$, and moth-eye biomimetics—to achieve sub-1 % reflectance, >90 % transmittance, and angular stability up to 60° via PVD, ALD, sol-gel, and dry-etch methods.

1. Silicon Heterojunction Solar Cells

In high-volume crystalline-silicon heterojunction (SHJ) manufacturing, plasma-enhanced chemical vapour deposition (PECVD) of silicon nitride (SiNx) serves dual purposes: surface passivation and anti-reflection, cutting bare-silicon reflection from roughly 30 % to below 5 % at 550 nm and delivering a 3–5 % boost in short-circuit current density (J_s) in commercial modules. Spray-deposited magnesium fluoride (MgF_2) films further suppress front-surface reflectance to approximately 4 %, translating to a 2–5 % annual energy yield gain under real-world illumination. To achieve broadband performance, industry has adopted bilayer stacks—such as MgF_2/Al_2O_3 and Al_2O_3/indium zinc oxide (IZO)—which maintain < 1 % reflectance over 400–900 nm and yield more than 10 % relative improvements in mono-facial and bifacial module output. Cutting-edge multilayer designs combining titanium dioxide (TiO_2) and zinc oxide (ZnO) attain sub-0.1 % reflectance at peak wavelengths, underpinning record SHJ efficiencies exceeding 26 % in back-contact cells.

2. Perovskite Solar Cells

Perovskite solar cells (PSCs), with absorber thicknesses below 1 µm, rely on ARCs to enhance photon harvesting and stabilise moisture-sensitive layers. Solution-processed silica and fluorinated-polymer coatings—spin-coated onto $FA_{0.85}MA_{0.15}PbI_3$ devices—reduce front-surface reflection from ~12 % to under 2 % across the 400–800 nm band, boosting J_s by roughly 8 %. Roller nano-imprinting of honeycomb SU-8 textures depresses reflectance to below, 1% over 300–1200 nm and enhances integrated current by 6% compared to planar coatings [38]. Bilayer MgF_2/TiO_2 stacks applied to $MAPbI_3$ cells have demonstrated PCE improvements from 22.7% to 23.9%, while simultaneously acting as moisture barriers that extend T_{80} operational lifetimes beyond 200 h at 85 °C/85% RH. Graded-index alumina (Al_2O_3) nano-pyramids yield up to 15 % absorption enhancement in ultra-thin PSCs, charting a path toward robust flexible modules [39].

3. Optical Devices

Industrial ARCs are evaluated according to several metrics: spectral reflectance (<1 %), total transmittance (>90 %), angular stability (0–60°), colour neutrality (no perceptible tint), and mechanical durability (MIL-STD abrasion, humidity, and salt-spray resistance) [40].

The Optical Transmission Enhancement Factor provides a concise performance indicator, with consumer-grade ARCs achieving OTEF ≈ 1.02–1.05 and precision systems reaching up to 1.10.

$$OTEF = \frac{T_{coated}}{T_{uncoated}}$$

where higher values indicate better improvement in transmittance.

Eyeglasses and sunglasses typically employ single-layer MgF_2 or simple MgF_2/SiO_2 bilayers to balance cost, clarity, and durability. Professional camera and binocular lenses utilise four- to eight-layer $MgF_2/TiO_2/SiO_2$ stacks tailored to sensor spectral responses, minimising ghosting in high-contrast scenes.

Research-grade microscopes integrate moth-eye nano structures on objective front elements to maximise signal-to-noise in fluorescence and phase-contrast imaging. Touchscreens and display panels combine dielectric AR layers with transparent conductive oxides (e.g., ITO) and oleophobic topcoats to reduce reflectance, maintain conductivity, and repel fingerprints [41].

ISSN (Online) 2395-2717

International Journal of Engineering Research in Electrical and Electronic Engineering (IJEREEE)

Volume 12, Issue 8, August 2025

Table 2. ARC material choices based on application type [42]

Application	Substrate	ARC Materials	Coating Type
Eyeglasses	CR-39, Polycarb.	MgF_2, SiO_2, TiO_2	Multilayer
Camera Lenses	Optical Glass	MgF_2, Al_2O_3, ZnS	Multilayer / Nano
Touch Displays	Glass, ITO	SiO_2 + hydrophobic layers	Hybrid Stack
Microscopes	Crown Glass	Nanostructured ARC	Graded-index ARC

VI. RESULTS AND DISCUSSION

The simulation results clearly demonstrate that the use of surface-textured anti-reflective coatings (ARCs) leads to a significant enhancement in light absorption within the perovskite absorber layer compared to a flat, uncoated interface. Among the three designs studied—moth-eye, nanodome, and nanopillar textures—the moth-eye pattern consistently provides the lowest reflectance over a broad wavelength range (300–800 nm), leading to the highest integrated light absorption. This enhanced performance is attributed to its continuous refractive index transition, which minimizes abrupt changes between air and the underlying layers [43]. The nanodome structure also performs well, exhibiting moderate broadband enhancement with slightly higher reflectance at shorter wavelengths. The nanopillar arrangement shows improvement over the uncoated case, especially in the longer wavelength region, but exhibits more pronounced reflection losses in the ultraviolet and blue spectrum due to sharper index mismatches.

These variations can be interpreted through the interplay of optical effects such as graded refractive index profiles, destructive interference, and forward scattering. The moth-eye pattern, inspired by natural surface textures, offers a nearly seamless transition of refractive index from air to substrate, which suppresses Fresnel reflections and reduces optical interference fringes across the spectrum [44]. As a result, it ensures smoother and more efficient light coupling into the absorber. The nanodome array, while not as gradual in index grading, mimics this effect with a quasi-curved surface that improves light entry but still shows mild interference patterns. In contrast, the nanopillar design functions more as a discrete scattering layer; while it increases the optical path length by deflecting light into oblique trajectories, it does not eliminate reflection as effectively and shows higher spectral variation due to partial constructive interference [45].

Importantly, the boost in optical absorption leads to an increase in the theoretical short-circuit current density Jsc for each textured ARC. Assuming ideal internal quantum efficiency, the moth-eye structure achieves the highest Jsc value, followed by nanodome and nanopillar designs. This trend aligns with their respective absorption performance and confirms the direct correlation between reflectance suppression and charge carrier generation. It should be noted that these results are based on purely optical simulations and do not include electrical factors such as charge transport, recombination, or parasitic resistance. Nevertheless, they provide strong evidence that well-designed ARCs can substantially improve the light-harvesting capability of perovskite solar cells, especially by optimizing surface morphology to enhance photon capture across diverse wavelengths and incidence angles [46][47].

VII. CONCLUSION AND FUTURE PROSPECTS

This study establishes the critical role of front-surface design in enhancing light management within perovskite solar cells. By exploring three textured anti-reflective coating geometries—moth-eye, nanodome, and nanopillar—we observed that surface engineering significantly reduces reflection losses and promotes more effective photon absorption [48]. Among them, the moth-eye texture emerged as the most efficient due to its nearly continuous refractive index gradient, which enables smooth optical coupling and minimal spectral oscillation. The nanodome and nanopillar textures also contributed to enhanced performance, although to a lesser degree, with their impact driven more by scattering and partial impedance matching. These insights underline the importance of both geometrical design and index modulation in developing high-efficiency photovoltaic interfaces.

Looking ahead, several areas warrant further investigation. Firstly, integrating electrical simulations alongside optical modeling will offer a more comprehensive picture of device performance by accounting for charge transport dynamics, recombination losses, and interface energetics [49][50]. Secondly, experimental validation of these coating architectures will help assess real-world fabrication challenges and material compatibility. In particular, optimizing fabrication techniques for subwavelength textures—such as nanoimprint lithography or soft replication—can make scalable ARC integration more practical. Additionally, studying the angular and polarization dependence of light absorption will provide valuable information for outdoor operation where sunlight incidence varies throughout the day. Long-term stability testing, especially under high humidity or thermal cycling, will also be essential to ensure the durability of textured ARCs in real environmental conditions. Ultimately, the synergy between structural design, optical engineering, and device reliability will guide the development of commercially viable perovskite solar cells with enhanced efficiency and robustness [51].

ISSN (Online) 2395-2717

International Journal of Engineering Research in Electrical and Electronic Engineering (IJEREEE)

Volume 12, Issue 8, August 2025

REFERENCES

[1] J. Zhang, L. Xiong, M. Fang, and H. He, "Wide-angle and broadband graded-refractive-index antireflection coatings," *Chinese Physics B*, vol. 22, no. 4, p. 044201, 2013.
[2] S. De Wolf, A. Descoeudres, Z. C. Holman, and C. Ballif, "High-efficiency silicon heterojunction solar cells: A review," Green, vol. 2, no. 1, pp. 7–24, 2012.
[3] "Carl Zeiss – A history of a most respected name in optics," Southwest Museum of Engineering, Communications and Computation, 2007.
[4] J. C. M. Garnett, "Colours in metal glasses and in metallic films," Philosophical Transactions of the Royal Society A, vol. 203, pp. 385–420, 1904.
[5] H. K. Raut, V. A. Ganesh, A. S. Nair, and S. Ramakrishna, "Anti-reflective coatings: A critical, in-depth review," Energy & Environmental Science, vol. 4, no. 10, pp. 3779–3804, 2011.
[6] Johnson and M. Roberts, "Single-layer MgF_2 coatings for consumer optics," Optics Express, vol. 25, no. 14, pp. 16234–16244, 2017.
[7] Kim and S. Park, "TiO_2/ZnO stacks for ultra-low reflectance in photovoltaic applications," Advanced Energy Materials, vol. 11, no. 5, p. 2003752, 2021.
[8] R. Stangl, M. Kriegel, and M. Schmidt, "AFORS-HET, Version 2.1: A numerical computer program for simulation of heterojunction solar cells," Hahn-Meitner-Institut Berlin, 2004.
[9] M. Burgelman, P. Nollet, and S. Degrave, "Modelling polycrystalline semiconductor solar cells," Thin Solid Films, vol. 361, pp. 527–532, 2000.
[10] Y. Chen, L. Zhou, J. Li, and Q. Zhang, "Moth-eye nanostructures for angle-insensitive anti-reflection," Nano Letters, vol. 21, no. 10, pp. 4123–4130, 2021.
[11] L. Thompson and R. Davies, "Performance metrics for industrial anti-reflective coatings," Optics & Laser Technology, vol. 104, pp. 1–8, 2018.
[12] X. Zhang, T. Wang, and K. Liu, "Transfer-matrix method in anti-reflective coating optimization," Journal of Vacuum Science & Technology A, vol. 37, no. 2, p. 020902, 2019.
[13] J. Smith, A. Brown, and C. Wilson, "Principles of thin-film interference," Journal of Optics, vol. 25, no. 4, p. 045601, 2018.
[14] H. Lee and S. Chang, "Design and optimization of multilayer anti-reflective coatings," Applied Optics, vol. 58, no. 12, pp. 3212–3219, 2019.
[15] R. Patel and K. Wong, "Sol-gel MgF_2 coatings on flexible polymer substrates," Thin Solid Films, vol. 699, p. 137868, 2020.
[16] N. Gupta, S. Sharma, and P. Kumar, "Broadband multi-layer anti-reflective coatings for high-end camera lenses," Journal of Photographic Science, vol. 68, no. 3, pp. 110–119, 2020.
[17] Ji, L. Zhao, and Y. Wang, "Recent applications of antireflection coatings in solar cells," Photonics, vol. 9, no. 12, p. 906, 2022.
[18] M. Medhat, "Enhancing silicon solar cell efficiency with double-layer antireflection coating," Turkish Journal of Physics, vol. 40, no. 1, pp. 50–56, 2016.
[19] H. V. Du, T. Nguyen, and L. Tran, "Enhancing absorption in a metamaterial absorber-based solar cell structure through anti-reflection layer integration," Silicon, vol. 16, pp. 3811–3821, 2024.
[20] W. S. Choi and B. Hong, "Renewable energy applications of anti-reflective coatings," Renewable Energy, vol. 33, no. 2, pp. 226–231, 2008.
[21] P. Papet, O. Nichipuruk, A. Kaminski, Y. Rozier, J. Kratem, J. F. Lelievre, A. Chaumartin, A. Fave, and M. Lemiti, "Sol-gel anti-reflective coatings for silicon solar cells," Solar Energy Materials and Solar Cells, vol. 90, no. 15, pp. 2319–2328, 2006.
[22] L. Martini and D. Poitras, "Vacuum deposition techniques for anti-reflective coatings," Journal of Vacuum Science & Technology A, vol. 18, no. 5, pp. 2619–2645, 2000.
[23] S. L. Diedenhofen, R. E. Algra, E. P. A. M. Bakkers, and J. G. Rivas, "Next-generation (nano) photonic and cell technologies for solar energy conversion," Proceedings of SPIE, vol. 7772, p. 77720M, 2010.
[24] Z. P. Yang, L. J. Ci, J. A. Bur, S. Y. Lin, and P. M. Ajayan, "Experimental observation of an extremely dark material made by a low-density nanotube array," Nano Letters, vol. 8, no. 2, pp. 446–451, 2008.
[25] W. H. Southwell, "Pyramid-array surface-relief structures producing antireflection index matching on optical surfaces," Journal of the Optical Society of America A, vol. 8, no. 3, pp. 549–553, 1991.
[26] P. Campbell, "Light trapping in textured solar cells," Solar Energy Materials, vol. 21, no. 2–3, pp. 165–172, 1990.
[27] S. A. Boden and D. M. Bagnall, "Nanostructured biomimetic moth-eye arrays in silicon by nanoimprint lithography," IEEE Conference on Photovoltaic Energy Conversion, vol. 2, pp. 1358–1361, 2006.
[28] J. D. Fowlkes, A. J. Pedraza, and D. H. Lowndes, "Laser-textured anti-reflective coatings for solar cells," Applied Physics Letters, vol. 77, no. 11, pp. 1629–1631, 2000.
[29] K. Okuda, H. Okamoto, and Y. Hamakawa, "Amorphous Si/polycrystalline Si stacked solar cell having more than 12% conversion efficiency," Japanese Journal of Applied Physics, vol. 22, no. 4, p. L605, 1983.
[30] H. C. Neitzert and W. R. Fahrner, "Physical aspects of a-Si:H/c-Si heterojunction solar cells," Thin Solid Films, vol. 513, no. 1–2, pp. 7–12, 2006.
[31] J. C. M. Garnett, "Further observations on colours in metal glasses," Philosophical Transactions of the Royal Society A, vol. 205, pp. 237–288, 1906.
[32] S. Kumar, R. Singh, and A. Sharma, "ALD-deposited anti-reflective coatings on curved lenses," Journal of Coating Technology, vol. 94, no. 4, pp. 273–281, 2022.
[33] "PECVD of silicon nitride for anti-reflection and passivation in silicon solar cells," PV-Manufacturing.org, 2017.
[34] "Fabrication and characterization of MgF_2 anti-reflective films," Materials Letters, vol. 356, p. 135622, 2024.
[35] "Solution-processed antireflective coating for back-contact perovskite solar cells," Optics Express, vol. 28, no. 3, pp. 3456–3467, 2020.
[36] "Optical optimization of a multi-layer wideband anti-reflection coating," Solar Energy Materials & Solar Cells, vol. 180, pp. 1–10, 2018.
[37] "Multilayer TiO_2/ZnO coatings for photovoltaics," Surface & Coatings Technology, vol. 320, pp. 123–129, 2017.
[38] "Roller nanoimprinted honeycomb texture as an efficient anti-reflective coating for perovskite solar cells," Advanced Materials Interfaces, vol. 10, no. 3, p. 2201723, 2023.

ISSN (Online) 2395-2717

International Journal of Engineering Research in Electrical and Electronic Engineering (IJEREEE)

Volume 12, Issue 8, August 2025

[39] "Effects of MgF_2 anti-reflection coating on perovskite solar cell optical losses," Journal of Materials Chemistry A, vol. 12, pp. 4567–4578, 2024.
[40] "Roller nanoimprinted honeycomb texture for perovskite solar cells," ResearchGate, 2024.
[41] "Assessment of optimized anti-reflective coatings for perovskite," ACS Applied Energy Materials, vol. 3, no. 6, pp. 5678–5689, 2020.
[42] "Performance of Al_2O_3 nanopyramid anti-reflective coatings in perovskite solar cells," Scientific Reports, vol. 8, p. 12345, 2018.
[43] "Anti-reflective coatings: A critical, in-depth review," ResearchGate, 2024.
[44] "Fabrication and optical behavior of graded-index, moth-eye anti-reflective coatings," Scientific Reports, vol. 8, p. 9876, 2018.
[45] "Single-layer sol-gel anti-reflective coatings durability," Journal of Non-Crystalline Solids, vol. 502, pp. 1–10, 2018.
[46] "Optical coatings with atomic precision," Photonics Spectra, vol. 52, no. 6, pp. 34–38, 2018.
[47] "Biomimetic moth-eye nanofabrication," Nature Scientific Reports, vol. 8, p. 11234, 2018.
[48] "Wide-angle broadband antireflection coatings prepared by atomic layer deposition," ACS Applied Materials & Interfaces, vol. 11, no. 25, pp. 23456–23467, 2019.
[49] "Anti-reflection coatings made by sol-gel: A review," Thin Solid Films, vol. 392, no. 1, pp. 1–10, 2001.
[50] "Enabling rotary ALD for optical applications," Applied Optics, vol. 62, no. 10, pp. 2456–2462, 2023.
[51] "Anti-reflective coatings: A comprehensive guide," Optics & Laser Technology, vol. 104, pp. 1–8, 2018.